

Investigation of the nuclear structure of $^{84-108}\text{Mo}$ isotopes using Skyrme-Hartree-Fock method

Ali A. Alzubadi, R. A. Radhi, Nabeel F. Latooffi

Department of Physics, College of Science, University of Baghdad

E-mail: ali.a.alzubadi@gmail.com

Abstract

Over the last few decades the mean field approach using self-consistent Hartree-Fock (HF) calculations with Skyrme effective interactions have been found very satisfactory in reproducing nuclear properties for both stable and unstable nuclei. They are based on effective energy-density functional, often formulated in terms of effective density-dependent nucleon–nucleon interactions. In the present research, the SkM, SkM*, SI, SIII, SIV, T3, SLy4, Skxs15, Skxs20 and Skxs25 Skyrme parameterizations have been used within HF method to investigate some static and dynamic nuclear ground state properties of $^{84-108}\text{Mo}$ isotopes. In particular, the binding energy, proton, neutron, mass and charge densities and corresponding root mean square radius, neutron skin thickness and charge form factor are calculated by using this method with the Skyrme parameterizations mentioned above. The calculated results are compared with the available experimental data. Calculations show that the Skyrme–Hartree–Fock (SHF) theory with above force parameters provides a good description on Mo isotopes.

Key words

Skyrme interaction, Skyrme-Hartree-fock method, Mo isotopes.

Article info.

Received: Sep. 2014

Accepted: Nov. 2014

Published: Apr. 2015

دراسة التركيب النووي لنظائر $^{84-108}\text{Mo}$ باستخدام طريقة السكيرم-هارتري فوك

علي عبد اللطيف الزبيدي، رعد عبد الكريم راضي، نبيل فوزي لطوفي

قسم الفيزياء، كلية العلوم، جامعة بغداد

الخلاصة

يتناول هذا البحث دراسة التركيب النووي لبعض نظائر $^{84-108}\text{Mo}$ من خلال حساب خواص الحالة الأرضية لها مثل كثافة كل من الشحنة، البروتون، النيوترون والكتلة مع انصاف الاقطار المرافقة لها وكذلك حساب السمك النيوتروني، طاقات الربط، وعوامل تشكل الشحنة. تم استخدام طريقة سكيرم هارتري فوك في تنفيذ هذه الدراسة مع بارامترات مختلفة وهي SkM, SkM*, SI, SIII, SIV, T3, SLy4, Skxs15, Skxs20, Skxs25 Skyrme. لقد تمت دراسة تأثير هذه البارامترات المختلفة على خواص النظائر المذكورة اعلاه وذلك لتحديد اي من هذه البارامترات يحقق افضل تطابق مع الحسابات العملية لتلك الخواص. ويستنتج من هذه الدراسة ان طريقة سكيرم هارتري فوك تعطي وصف جيد لخواص هذه النظائر. كما تمت المقارنة بين النتائج النظرية والتجريبية لعوامل تشكل الشحنة.

Introduction

Over the last ten years, Hartree-Fock (HF) calculations using phenomenological density-dependent effective forces like

Skyrme forces have been found very satisfactory in reproducing static and low energy dynamical nuclear properties [1]. It is a very useful tool for the calculations of

the mean field approach which assumes that nucleons move independently in a mean field generated by the other nucleons of the atomic nucleus. They produce the appropriate single-particle potential corresponding to the actual density distribution for a given nucleus based on nucleon–nucleon interactions. The most prominent interaction used with the HF method is the Skyrme interaction. The Skyrme-Hartree-Fock (SHF) theory has been proved to be very successful for the description of the ground state properties of both stable and unstable nuclei since the implementation of the Skyrme interaction by Vautherin and Brink [1-3]. It incorporates the essential physics in terms of a minimal set of parameters, e.g., an s - and p -wave expansion of an effective nucleon–nucleon interaction together with a density dependent part which accounts for the truncation of the shell–model space to a closed-shell configuration as well as for three-body interactions. A common trend of phenomenological interactions used in the mean field approach is their simple mathematical structure. It has mathematically a zero range; however, velocity dependent terms mock up the finite range of the nuclear force. This allows writing the nuclear part of the HF energy as a functional of *local* one-body densities only, and the HF equations take the form of simple Schrödinger equations with local mean fields [4].

The structure of a nucleus can be described in nuclear physics by calculating some of the basic quantities such as various nuclear densities and the associated root-mean-square (rms) radii, the neutron-skin thickness and charge form factors. Nuclear charge density distribution gives us much detailed information on the internal structure of nuclei since they are directly related to the wave functions of protons, which are

important keys for many calculations in nuclear physics [5, 6].

In the present research, we will investigate some static and dynamic ground state properties of $^{84-108}\text{Mo}$ isotopes using ten typical parameterizations of SKM, SKM*, SI, SIII, SVI, TIII, SLy4, Skxs15, Skxs20 and Skxs25 [7-13].

Theory

The effective interaction proposed by Skyrme was designed for HF calculations of nuclei [14, 15]. It is the most convenient force used in the description of the ground state properties of nuclei with about ten adjustable parameters which are obtained by fitting the experimental data of nuclei, such as binding energies and charge radii [16]. The Skyrme forces are zero-range interactions, it is basically consist of a two-body term which is momentum dependent and a zero range three-body term. In the HF calculations, the three-body term can be replaced with a density-dependent two-body term. Thus, the Skyrme forces are unified in a single form as an extended Skyrme force [17]. The two-body Skyrme interaction is written as follows [14]:

$$\begin{aligned}
 v_{12} = & t_0(1 + x_0 \beta_\sigma) \delta(r_1 - r_2) \\
 & + \frac{1}{2} t_1 (1 + x_1 \beta_\sigma) (\vec{k}^2 \delta(r_1 - r_2) + \delta(r_1 - r_2) \vec{k}^2) \\
 & + t_2 (1 + x_2 \beta_\sigma) \vec{k}^2 \cdot \delta(r_1 - r_2) \vec{k} \\
 & + \frac{1}{6} t_3 (1 + x_3 \beta_\sigma) \rho^\alpha(\vec{R}) \delta(r_1 - r_2) \\
 & + W_0 \vec{k}(\sigma_1 + \sigma_2) \times \vec{k} \delta(r_1 - r_2),
 \end{aligned} \tag{1}$$

where the $\vec{k} = (\nabla_1 - \nabla_2)/2i$ and $\vec{k}' = -(\nabla_1' - \nabla_2')/2i$ operators are the relative wave vectors of two nucleons acts to the right and to the left (*i.e.* the complex conjugate wave functions, with coordinate r') [18], respectively. The terms $t_0, t_1, t_2, t_3, x_0, x_1, x_2, x_3$ and W_0 are the free

parameters describing the strengths of the different interaction terms which are fitted to the nuclear structure data. \vec{P}_σ is spin-exchange operators. $\delta(r_1 - r_2)$ is the Dirac delta function, and σ is the Pauli spin matrices.

The total-energy density of a nucleus in the standard SHF model, is written as [18]

$$E = E_{kin} + E_{Sky} + E_{Coul} + E_{pair} + E_{cm} \quad (2)$$

where E_{kin} is the kinetic energy of the nucleons (proton and neutron) which are given by the following relation [19]:

$$E_{kin} = \sum_{i=1}^A \frac{\hbar^2}{2m_i} \int d^3r \tau_i \quad (3)$$

E_{Sky} is the energy functional of the Skyrme force and given by:

$$E_{Sky} = \int d^3r \left[\frac{b_0}{2} \rho^2 - \frac{b_0'}{2} \sum_q \rho_q^2 + \frac{b_3}{3} \rho^{\alpha+2} - \frac{b_3'}{3} \rho^\alpha \sum_q \rho_q^2 + b_1 \rho \tau - b_1' \sum_q \rho_q \tau_q - \frac{b_2}{2} \rho \Delta \rho + \frac{b_2'}{2} \sum_q \rho_q \Delta \rho_q - b_4 \rho \nabla \cdot J - b_4' \sum_q \rho_q \nabla \cdot J_q \right] \quad (4)$$

where ρ_q is the local densities for protons and neutrons (depending on the value of q), ρ the total density, τ_q is the kinetic energy densities for protons and neutrons, α is Skyrme force parameter and J_q is the spin-orbit current density. They are given by [3]:

$$\rho_q(r) = \sum_{i\sigma} |\phi(r, \sigma, q)|^2, \quad \tau_q(r) = \sum_{i\sigma} |\nabla \phi(r, \sigma, q)|^2, \quad J_q(r) = -i \sum_{i\sigma} \phi_i^*(r, \sigma, q) [\nabla \phi_i(r, \sigma', q) \times \langle \sigma | \sigma' | \sigma \rangle] \quad (5)$$

The parameters in the Skyrme energy equation are given by:

$$\begin{aligned} b_0 &= t_0 \left(1 + \frac{1}{2} x_0 \right), & b_0' &= t_0 \left(\frac{1}{2} + x_0 \right) \\ b_1 &= \frac{1}{2} \left[t_1 \left(1 + \frac{1}{2} x_1 \right) + t_2 \left(1 + \frac{1}{2} x_2 \right) \right] \\ b_1' &= \frac{1}{2} \left[t_1 \left(\frac{1}{2} + x_1 \right) - t_2 \left(\frac{1}{2} + x_2 \right) \right] \\ b_2 &= \frac{1}{8} \left[3t_1 \left(1 + \frac{1}{2} x_1 \right) - t_2 \left(1 + \frac{1}{2} x_2 \right) \right] \\ b_2' &= \frac{1}{8} \left[3t_1 \left(\frac{1}{2} + x_1 \right) + t_2 \left(\frac{1}{2} + x_2 \right) \right] \\ b_3 &= \frac{1}{4} t_3 \left(1 + \frac{1}{2} x_3 \right), \\ b_3' &= \frac{1}{4} t_3 \left(\frac{1}{2} + x_3 \right). \end{aligned} \quad (6)$$

The third part of the total energy equation is the Coulomb energy part. There is a small contribution to the Coulomb energy coming from the exchange part. This contribution is due to the fact that the Coulomb interaction is of infinite range [2, 20]. The Coulomb energy is given by:

$$E_{Coul} = \frac{e^2}{2} \iint \frac{\rho_p(r) \rho_p(r')}{|r - r'|} dr dr' + E_{Coul\text{exch}} \quad (7)$$

$$E_{Coul\text{exch}} = -\frac{3}{4} e^2 \left(\frac{3}{\pi} \right)^{1/3} \int \rho_p(r)^{4/3} dr \quad (8)$$

In the SHF theory using the Skyrme forces, the most general product wave functions (φ_i) consist of independently moving single particles. In this method the neutron and proton densities are given by [1]:

$$\rho_q(\vec{r}) = \sum_i |\varphi_i(r)|^2 = \sum_\beta w_\beta \frac{2j_\beta + 1}{4\pi} \left(\frac{R_\beta}{r} \right)^2. \quad (9)$$

Here, q denotes the neutron or proton and w_β represents the occupation weight of single-particle levels. The completely filled shells have $w_\beta = 1$, but fractional occupancies occur for non-magic nuclei.

We restrict ourselves to considering the ground state of spherical nuclei.

The root-mean-square (rms) radii of neutron, proton, charge and mass distributions can be evaluated from these density distributions by [21]:

$$r_q = \langle r^2 \rangle^{1/2} = \left[\frac{\int r^2 \rho_q(r) dr}{\int \rho_q(r) dr} \right]^{1/2} \quad (10)$$

The thickness of a neutron skin is a very sensitive probe of the pressure difference that exists between neutrons and protons in the atomic nucleus. In nuclei it may be defined as the difference between the neutron and proton diffraction radii

$$t = \langle r^2 \rangle_n^{1/2} - \langle r^2 \rangle_p^{1/2} \quad (11)$$

The proton and neutron densities from the HF method with the intrinsic charge density of the nucleons can be calculated as a simple product in Fourier space, so as to transform the densities to the so-called form factors [22]

$$F_{ch}(q) = 4\pi \int_0^\infty dr r^2 j_0(qr) \rho_{ch}(r) \quad (12)$$

where q is the momentum transfer, and $j_0(qr) = \sin qr / qr$ is the spherical Bessel function of zeroth order. The normalization in Eq. (12) was chosen to give $F_{ch}(q=0) = 1$

Results and discussion

The Skyrme parameterizations that have been used in the present research were tabulated in Table I. We first calculate binding energies, the charge rms radii, and the neutron Skin thickness, then the charge, proton, neutron and mass densities are presented using the best Skyrme parameterization which gives the best reproduction of the binding energy data. These calculations are followed by the investigation of the longitudinal form factor for the Mo-isotopes using the same Skyrme parameterizations mentioned above.

Fig.1 shows the charge density profiles obtained with the investigated Skyrme parameterizations used in this work as well as the experimental charge distributions for ^{92}Mo [12, 20]. Theoretically, the calculated charge density values are quite consistent with the theoretical calculations with all the Skyrme parameterizations. In general, theoretical and experimental charge densities agree nicely in the fall-off region and differ more in the nuclear interior as a consequence of the shell oscillations of the mean-field densities specially for SkM*, SI, SIII, and SVI. For the other Skyrme parameterizations the theoretical calculations coincide with the experimental data for all the range of r (fm).

Since the nucleons themselves have intrinsic electromagnetic structure, the proton and neutron densities have been studied to compute the observable charge density from the HF results. Fig.2 shows the charge, proton, neutron and mass densities for the $^{84-108}\text{Mo}$ isotopes calculated with SkM Skyrme parameterization.

From Fig.2 (a) we note that the central nuclear charge densities gradually decrease as the neutron number increases. This is due to the change in the self-consistent HF potential coming from the additional neutrons. This change in charge density is available in the interior and the surface regions of the nuclei. The contribution of additional neutrons to the density is directly associated to the orbits that are filled. In $^{84-108}\text{Mo}$, the added neutrons fill the shells $1g_{9/2}$, $1g_{7/2}$ and $2d_{5/2}$. These orbits are changing the densities in the interior and the surface regions. For this reason the neutron densities in Fig.2 (c) are different for the Mo isotopes for all region of r (fm).

Table I: The Skyrme parameterizations that have been used in the present research.

	(1)	(2)	(3)	(4)	(5)	(6)	(7)	(8)	(9)	(10)
	SkM*	SkM	SI	SIII	SVI	SLy4	TIII	Skxs15	Skxs20	Skxs25
t_0	-2883.29	-2883.29	-2883.29	-2883.29	-2883.29	-2488.9	-2883.29	-2883.29	-2883.29	-2883.29
t_1	385.0	410.0	235.9	395.0	271.67	486.8	298.5	291.6	302.73	315.5
t_2	-120	-135	-100	-95	-138.33	-546.3	-99.05	-314.89	-323.42	-329.3
t_3	15595	15595	14463.5	14000	17000	13777	12794	18239.55	18237.49	18229.81
W_0	130	130	0.0	120	115	123.0	126	161.35	162.73	136.93
x_0	0.09	0.09	0.56	0.45	0.583	0.834	0.138	0.4762	0.13746	-0.18594
x_1	0.0	0.0	0.0	0.0	0.0	-0.344	-1.0	-0.25433	-0.25548	-0.24766
x_2	0.0	0.0	0.0	0.0	0.0	-1.0	1.0	-0.61109	-0.60744	-0.60119
x_3	0.0	0.0	1.0	1.0	1.0	1.354	0.075	0.52936	0.05428	-0.40902
α	1/6	1/6	1.0	1.0	1.0	1/6	1/3	1/6	1/6	1/6

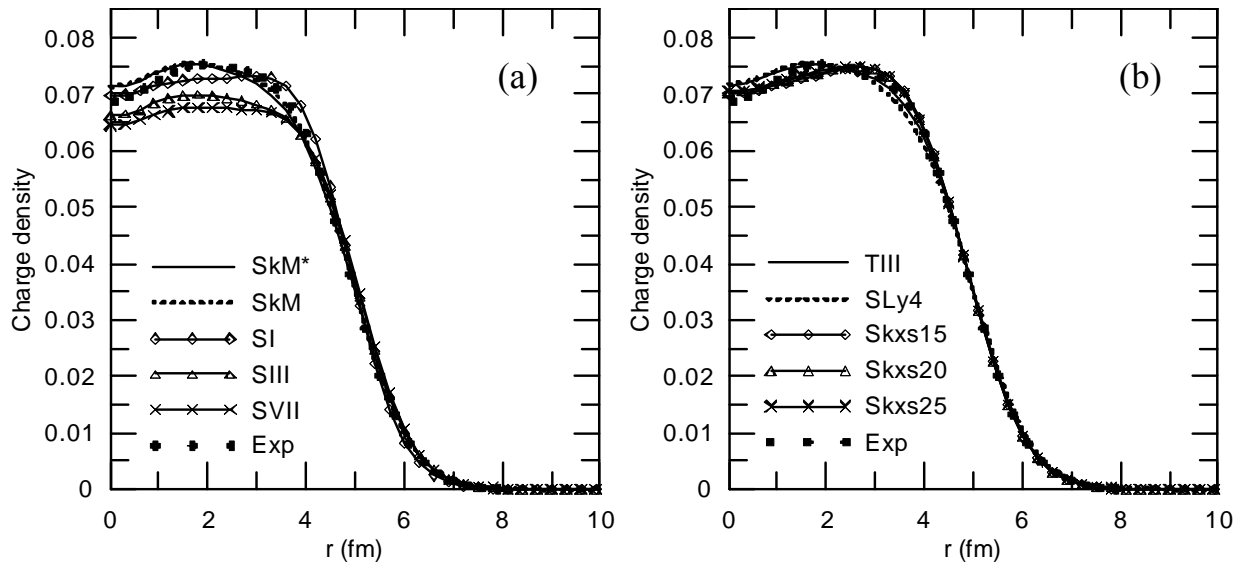


Fig.1: Charge density distribution for ^{92}Mo using different Skyrme parameterizations.

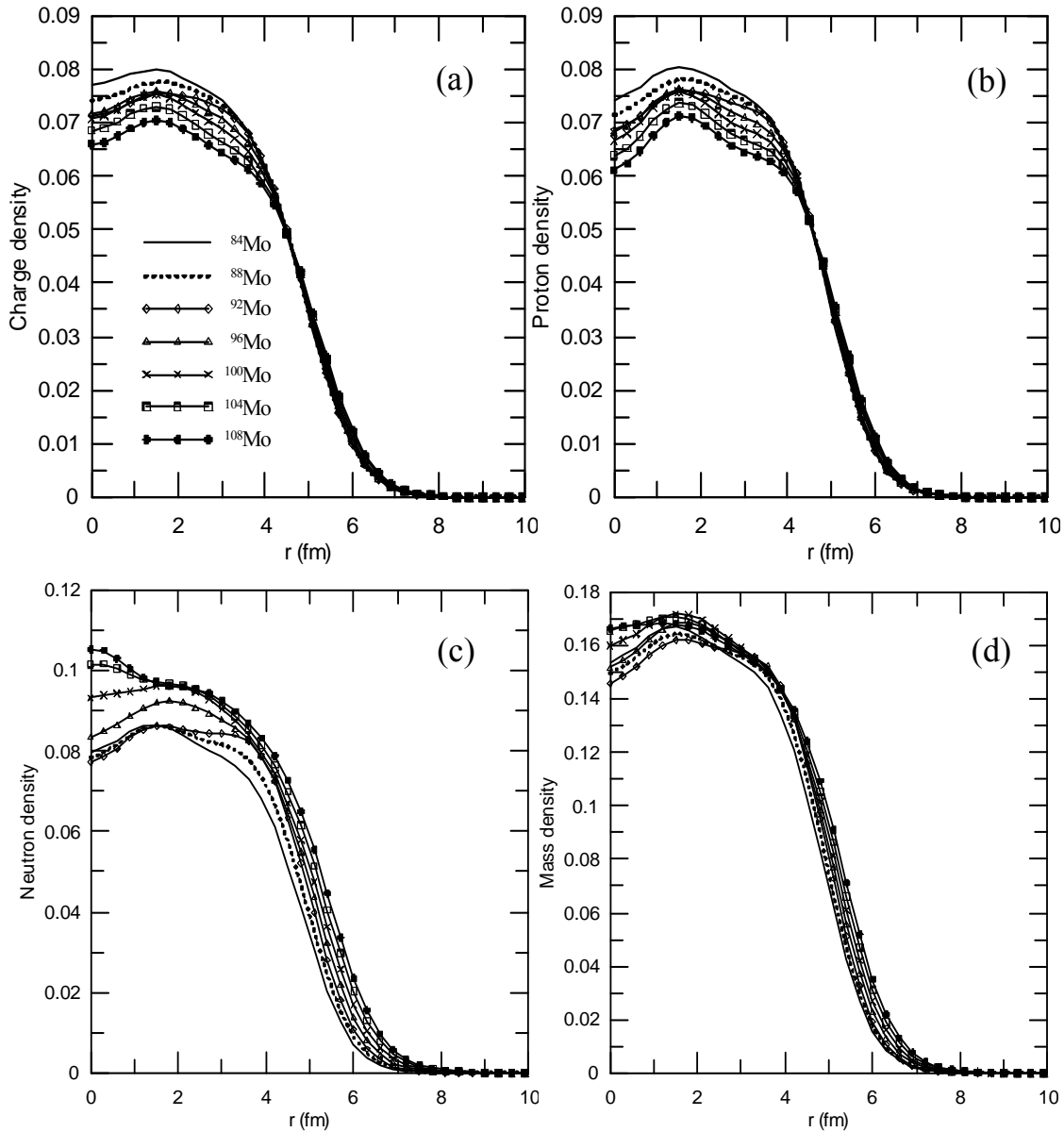


Fig.2: The density distribution of the $^{84-108}\text{Mo}$ isotopes using SkM Skyrme parameterization. (a) charge density, (b) proton density, (c) neutron density and (d) mass density.

The calculated binding energies per particle for $^{84-108}\text{Mo}$ isotopes as a function of the mass number along with those of experimental data are shown in Fig. 3. It may be seen from this figure that

calculated binding energies agree remarkably well with the experimental ones [23- 25], and are in fact very close to those obtained from interactions SkM for Mo isotopes.

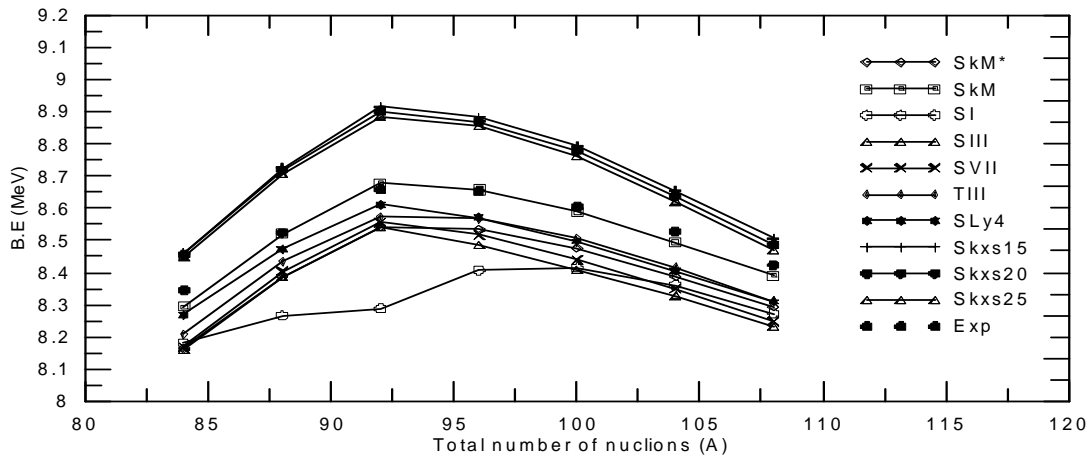


Fig.3: The total binding energy per nucleon for $^{84-108}\text{Mo}$ isotopes using different Skyrme parameterizations within HF method.

The obtained rms charge radii and neutron skin thicknesses are plotted in Figs. 4 and 5. The calculated rms charge radii for $^{84-108}\text{Mo}$ isotopes obtained with all the selected parameters are compared with the experimental data [26, 27]. The best rms charge radii are obtained with SLy4 and SkM*. For the neutron skin thickness (t), it can be seen from Fig. 5 that the theoretical values of t increase with increasing mass number. Its values increased from -0.08 fm (for ^{84}Mo) to

0.256 fm (for ^{108}Mo) by increasing the neutron number. The difference between the rms radii of neutrons and protons for $N = Z$ nuclei, or for nuclei with a small neutron excess is negative as one should expect, the Coulomb force pushes the protons away. Since there exist only few reliable data for neutron radii, especially for nuclei with a small neutron excess, the comparison of the neutron skin thickness with experiment is difficult.

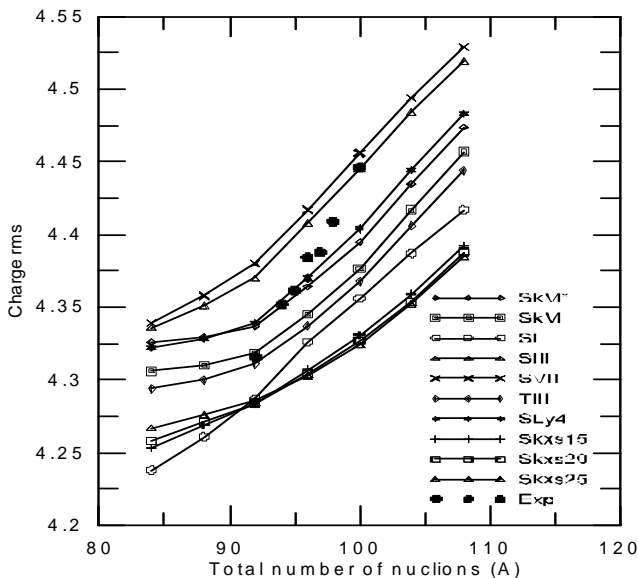


Fig.4: The calculated rms charge radii for $^{84-108}\text{Mo}$ isotopes using different Skyrme parameterizations.

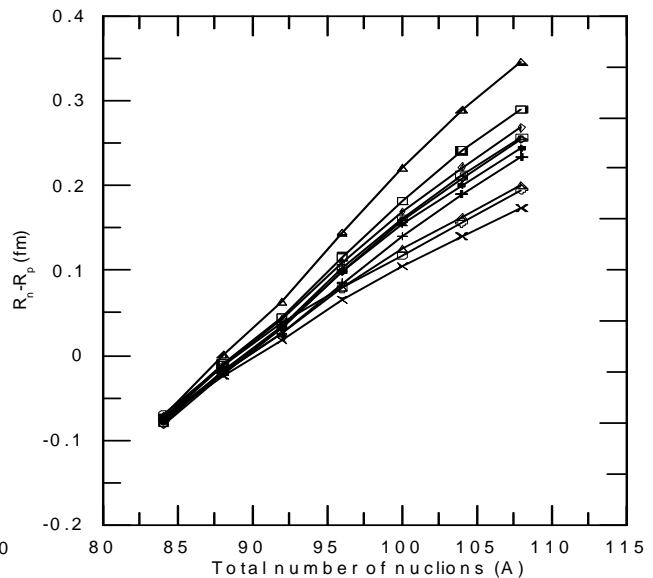


Fig.5: The neutron skin thickness t for $^{84-108}\text{Mo}$ isotopes against the mass number using different Skyrme parameterizations.

The calculated and experimental rms charge radii as well as the proton and neutron rms radii for the stable ^{92}Mo using different Skyrme parameterizations are shown in Fig. 6. It can be seen from this comparison that the best Skyrme parameterizations are the SkM and SLy4.

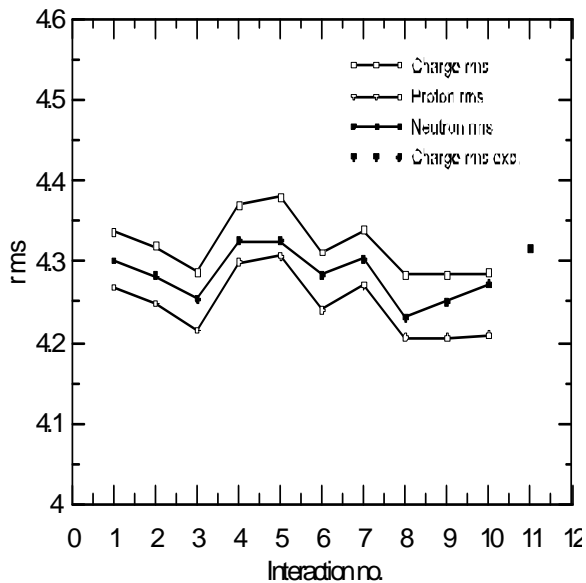


Fig.6: The calculated proton and neutron rms radii for ^{92}Mo nucleus using different Skyrme parameterizations.

A study of the charge-density distributions cannot be completely considered without the form factors, since the latter are an important quantities measured experimentally. Thus, in Fig.7, for comparison we plotted the charge form factor for the stable ^{92}Mo nucleus using SkM, SkM*, SLy4, Skxs15, Skxs20 and Skxs25 Skyrme parameterizations with the experimental data. The circles for the experimental data are given only over the range of momentum transfers measured experimentally. The plane-wave form factors $|F(q)|^2$ in these figures are

associated with the densities in Figs.1 (a) and (b), where the form factors in the range of moderate momentum transfer are sensitive to the change of the tail part of the charge density [28], while small q (fm^{-1}) values inform on the surface shape. It is apparent from Fig.7 that the theoretical curves (solid) and the experimental ones [29] (filled circles) for ^{92}Mo almost coincide in the range of low and moderate-momentum transfer q (fm^{-1}) out to about 1.75 fm^{-1} . The deviation occurs between the theoretical form factor and the experimental one at high momentum transfers. Since the form factor in this range of momentum transfer is mainly sensitive to the details of the inner part of the charge density distribution, its occurrence indicates that the theoretical charge density distribution has a departure from the experimental one around the center of the nucleus. Disagreement between experiment and theory above 1.75 fm^{-1} (and the associated discrepancies in the charge densities) might be related to two factors; first, the Skyrme interaction is a low-momentum expansion of the effective interaction, and one must expect the density fluctuations resulting from this approximation to break down at some point. Second, the mesonic-exchange corrections to the charge form factor become increasingly important at higher momentum transfers [30].

We also investigate in Fig.8 the charge form factor for the $^{84-108}\text{Mo}$ isotopes using the Skxs25 Skyrme parameterization. These figures show the behavior of the charge form factor with the increasing neutron numbers, which is associated with the charge density of the $^{84-108}\text{Mo}$ isotopes in Fig.2 (a).

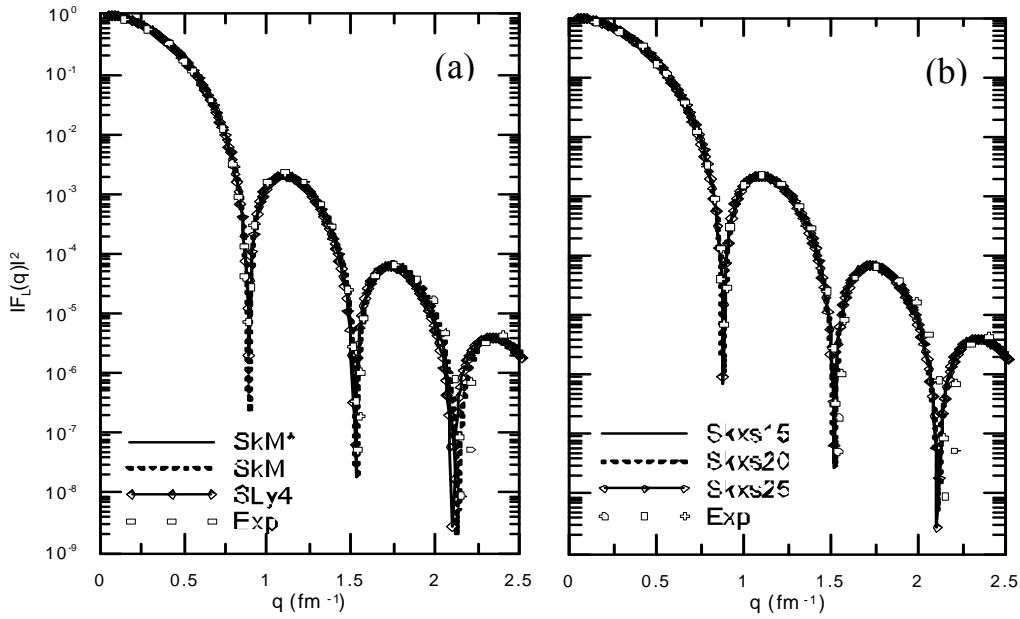


Fig. 7: The charge forms factor for ^{92}Mo versus momentum transfer q (fm^{-1}) using different Skyrme parameterizations.

According to the charge form factors shown in Fig. 2 (a), we can see that the minima shift upward and inward with an increasing neutron number. This trend of change is due to the variation in the

nuclear charge densities, especially the mainly due to the enhancement of the proton densities in the peripheral region and also to the contribution of the charge distribution of the neutrons themselves.

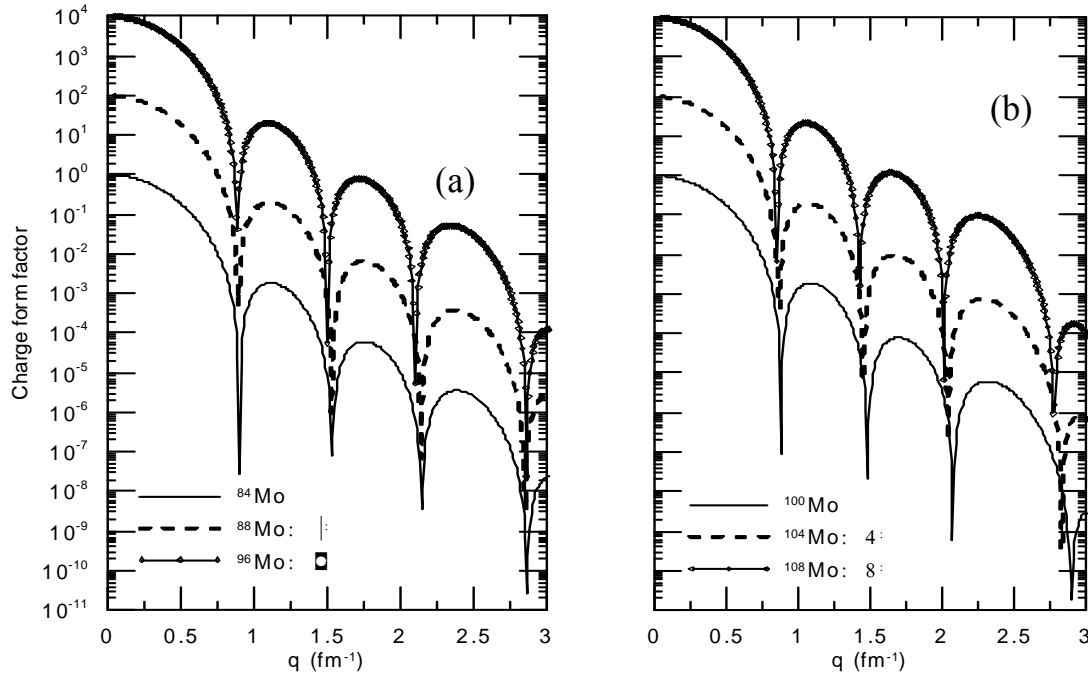


Fig. 8: The charge forms factor for $^{84-108}\text{Mo}$ isotopes versus momentum transfer q (fm^{-1}) using Skxs25 Skyrme parameterization.

Conclusions

In the present research, we have investigated the nuclear ground state properties such as the binding energies per particle, charge, neutron and proton density distributions and the associated rms radii, neutron skin thicknesses and charge form factor for $^{84-108}\text{Mo}$. The conclusions drawn from this investigation are as follows:

- 1- The Skyrme-Hartree-Fock method is useful for spherical nuclei because the Skyrme force is central and has zero range.
- 2- The B.E. of $^{84-108}\text{Mo}$ calculated using the SHF method with the SkM parameterization is in closer agreement with the experimental data.
- 3- The calculated charge rms radii for ^{92}Mo with SkM and Sly4 parameterizations are closer to the experimental data.
- 4- The neutron skin thickness t increases with the neutron number for Mo isotopes.
- 5- The charge form factor obtained using SkM parameter much more coincides with the experimental data especially in the range of momentum transfer up to 1.75 fm^{-1} .

References

- [1] T. Siiskonen, P. O. Lipas, J. Rikowska, Phys. Rev. C60 (1999) 034312.
- [2] D. Vautherin and D. M. Brink, Phys. Rev. C5 (1972) 626.
- [3] J.R. Stone, P.G. Reinhard, Progress in Particle and Nuclear Physics, 58 (2007) 587.
- [4] M. Zamrun, I. Usman, L. Aba, Journal Matematika Dan Sains, 16 (2011) 58.
- [5] E. Tel, S. Okuducu, G. Tanir, N. N. Akt, M.H. Bolukdemir, Commun. Theor. Phys. 49 (2008) 696.
- [6] R. Hofstadter, Rev. Mod. Phys. 28 (1956) 214.
- [7] J. Bartel, P. Quentin, M. Brack, C. Guet, H. B. Hakansson, Nucl. Phys. A386 (1982) 79.
- [8] M. Brack, C. Guet, H. B. Hakansson, Phys. Rep. 123 (1985) 275.
- [9] E. Chabanat, P. Bonche, P. Haensel, J. Meyer, R. Schaeffer, Nucl. Phys. A635 (1998) 231.
- [10] G. Q. Li, J. Phys. G. Nucl. Part. Phys. 17 (1991) 1.
- [11] E. Tel, H. M. Sahin, A. Kaplan, A. Aydin, T. Altinok, Ann. Nucl. Energy 35, 2 (2007) 220.
- [12] E. Tel, S. Okuducu, G. Tanir, N. Nur Akti, M.H. Bolukdemir, Commun. Theor. Phys. 49 (2008) 696.
- [13] B. Alex Brown, G. Shen, G. C. Hillhouse, J. Meng, A. Trzcinska, Phys. Rev. C76 (2007) 034305.
- [14] T. H.R. Skyrme, Nucl. Phys. 9 (1959) 615.
- [15] T. H. R. Skyrme, Philos. Mag. 1 (1956) 1043.
- [16] M. Bender, P. H. Heenen, P. G. Reinhard. Rev.Mod. Phys. 75 (2003) 121.
- [17] H. Aytakin and D. Demirbag, Indian J. Phys. 13 (2013) 0253.
- [18] E. Tel, A. Aydin, A. Kaplan, B. Sarer, Phys. Rev. C 77 (2008) 054605.
- [19] J. Erler, P. Klupfel, P. G. Reinhard, J. Phys. G: Nucl. Part. Phys. 38 (2011) 033101.
- [20] M. Beiner, H. Flocard, Nguyen Van Giai, and P. Quentin, Nucl. Phys. A238 (1975) 29.
- [21] H. Aytakin, E. Tel, R. Baldik, A. Aydin, J. Fusion Energy, 30 (2011) 21.
- [22] C. A. Bertulani, J. Phys. G: Nucl. Part. Phys. 34 (2007) 315.
- [23] B. Dreher, J. Friedrich, K. Merle, H. Rothhaas, G. Lührs, Nucl. Phys. A235 (1974) 219.
- [24] H. Vries, C. W. Jager, C. Vries, At. Data Nucl. Data Tables 36 (1987)495.

- [25] G. Fricke, C. Bernhardt, K. Heiling, L. A. Schaller, L. Shellenberg, E. B. Shera, C. W. de Jager, *At. Data Nucl. Data Tables*, 60 (1995) 177.
- [26] I. Angeli, *At. Data Nucl. Data Tables* 87 (2004) 185.
- [27] I. Angeli, K.P. Marinova, *At. Data Nucl. Data Tables* 99 (2013) 69.
- [28] D. Durand, E. Suraud, B. Tamain "Nuclear Dynamics in the Nucleonic Regime" (IOP publishing, London, ltd 2001).
- [29] P. Finelli, N. Kaiser, D. Vretenar, W. Weise, *Nucl. Phys. A770* (2006) 1.
- [30] J. W. Negele, D.O. Riska, *Phys. Rev. Lett.* 40 (1978) 1005.